Egyptian Journal of Chemistry
http://ejchem.journals.ekb.eg/

Comparative Study of Electrochemical Corrosion of Novel Designs of 90/10 and 70/30 Copper-Nickel Alloys in Brine Solutions

Ghalia A. Gaber*, Walaa A. Hussein, Amal S. I. Ahmed
Chemistry Department, Faculty of Science (Girls), Al-Azhar University, Nasr City, Cairo, Egypt.

COPPER-NICKEL alloy is a material of choice for condensers and heat exchangers, where seawater is used as a coolant and in desalination plants. In this work, we survey the comparative corroding behavior of novel designs of 90/10 and 70/30 Copper-Nickel alloys under higher salinity (3.5 wt%, 10 wt% and 15 wt% NaCl). The electrochemical corrosion of Cu-Ni alloys in brine solutions was studied using potentiodynamic polarization, chronoamperometric and electrochemical impedance spectroscopy measurements along with scanning electron microscope (SEM) and energy dispersive X-Ray analyzer (EDX) investigations. Polarization data showed that Cu-10 Ni alloy is more corrosive than Cu-30 Ni alloy in 3.5 wt% NaCl solutions. Chronoamperometric curves confirmed the results obtained by polarization measurements that the uniform and pitting corrosion of Cu-Ni alloy were reduced in the Cu-30 Ni alloy in 3.5wt% NaCl solutions. Impedance spectra revealed that the surface and polarization resistances recorded higher values in Cu-30Ni alloy. SEM/EDX investigations indicated that the corrosion of Cu-Ni alloys proceeded by the selective electro-dissolution of nickel, which allowed copper enrichment on the surface of the alloy. The heat exchanger served to heat desalinated water, the water had a high chloride level. Corrosion examination indicated susceptibility towards pitting corrosion, especially at high temperature.

Keywords: Corrosion, Cu-Ni Alloys, Brine Solutions, Electrochemical Techniques, Spectroscopic analysis.

Introduction

The copper-nickel alloys are one of the major materials used in marine engine condenser piping systems including coastal power plants, desalination plants, line conditioning plant, bases for heat exchangers and condensers together with feed water system heaters, pipelines in shipbuilding, oil tank, paper machine construction, food and drink industry, power stations, chemical industry for fittings, valve fittings, pumps, measuring instruments, stirrer, filling plant, steamship and deep-sea submergence equipment, due to their good mechanical workability, good resistance to chloride erosion, high thermal conductivity and useful resistance to fouling [1]. The interest group in studying the electrochemical corrosion and characteristics of Cu-Ni alloys are because of their good corrosion resistance and the resistance of copper alloys to biological residues. Therefore, most of the studies focused on their behavior in the marine environment which, failure of Cu-Ni alloys mainly occurs at the surface, which seriously affects the safe surgery of ships and offshore engineering systems. Therefore, it has become an important engineering issue to further improve the corrosion resistance of these alloys in order to prolong the help life of the alloys and prevent early failure to better service marine engineering [2]. In large cities on the beach, various levels of water salinity are used in various water cooling systems. The salinity of seawater varies subject to local status, where it is affected by ambient and topographical conditions. For example, enclosed seas have a higher salinity than clear seas and oceans. Also, seas, which are found in expanse of high temperatures or that receive high drainage rates of saline water, would

certainly have a higher degree of salinity. This is because of a large amount of water received from river and spring in that area [3].

So, corrosion is expected to occur on the side of the heat exchange tubes which the water contains quite hights chloride levels which are due to the use of desalinated water [4]. Studies were perfect in chloride [5, 6], in either natural or synthetic sea water, in the absence or presence of sulfide to understand the corrosion mechanism under different conditions. The corrosion of copper–nickel alloys in natural seawater and in solution containing chloride ions has been investigated by many authors [1]. Copper-nickel alloys are widely used in marine environments due to their resistance to corrosion in saline solutions. Although the first corrosion rate of copper and its alloys may be high, it decreases as protective product layers are formed. The corrosion resistance provided by a layer of reaction product varies according to the alloy and the constitution of the electrolytic solution, and the thickness and electrical property of a passive film are dependent on this composition [7]. These studies also uncovering that the corrosion rate of the Cu-Ni alloys decreases sharply with increasing nickel content in the alloy. It was reported that the increase of Ni content improves the corrosion resistance of the alloy at high chloride concentration [5]. The plus of nickel to copper improves its strength and durability and also the resistance to corrosion, erosion, and cavitation in all natural waters including sea-water and brackish, treated or polluted waters. The heading of this article is to discuss normal applications for copper-nickel alloys and the reasons for their choice. The present work will address a problem of great importance to the local and regional industries (e.g. desalination, refining, power generation …etc). We study corrosion behavior of novel designs of 90/10 and 70/30 Copper-Nickel alloys under higher salinity (3.5 %, 10 % and 15 % NaCl).

Experimental

Two types of Cu-Ni alloys used in this study having the chemical composition (wt %) are shown in Table 1. Prior to each experiment, the working electrode was polished with different grades of emery paper up to 1200 grit, rinsed with acetone and finally with doubly distilled water. The auxiliary electrode was platinum wire, while a reference electrode Ag/AgCl (0.197 V SHE),

connected to a conventional electrolytic cell of capacity 50 ml. The experiments were studied the corrosion behavior of novel designs of Copper-Nickel alloys under higher salinity (3.5 wt%, 10 wt% and 15 wt% NaCl). All solutions were freshly prepared using analytical grade reagents and doubly distilled water. All experiments were performed at a required temperature (25 ± 1 °C). Three different electrochemical methods were used to evaluate the corrosion behavior of Cu-Ni alloys. The potentiodynamic polarization, chronoamperometric current-time (CT) measurements, and Electrochemical Impedance Spectroscopy (EIS) were performed using the Voltalab 40 Potentiostat PGZ301 made in Germany. The Volta Master 4 software was designed to measure and analyze the corrosion rate.

The potentiodynamic polarization of Cu-Ni alloys was carried out at range of potential from (-800 to 1000 mV$_{Ag/AgCl}$) and scan rate 2 mV/s., then Tafel lines were plotted and the different corrosion parameters such as corrosion rate (C.R), corrosion potential (E_{corr}) and corrosion current density (I_{corr}) values were recorded.

Chronoamperometric potentiostatic current-time (CT) technique applied a constant potential to the metal solution interface and measured its electrochemical behavior as a function of time. Potentiostatic experiments can be used to determine diffusion coefficients of dissolved materials in a solution to measure passivation or re-passivation potentials and to evaluate anodic and cathodic protection techniques. From the potentiodynamic curves, a certain electric potential in the passive region was selected and specimens of the tested alloys were potentiostatically polarized to this potential and kept at this potential for 35 min.

The impedance measurements of the Cu-Ni alloys were carried out in frequency range from (100 kHz to 100 mHz) with amplitude of 10 mV peak-to-peak using ac signals at open circuit potential. The SEM images were obtained by using SEM Model Quanta 250 FEG (Field Emission Gun) attached with EDX Unit (Energy Dispersive X-ray Analyses), with accelerating voltage 30. SEM and EDX analyses were used to define the morphology of surface attack and the chemical composition of corrosion products on Cu-Ni alloys from testes terminated just after the film breakdown occurred.

Results and Discussion

Electrochemical corrosion of Cu-Ni alloys in brine solutions

Potentiodynamic polarization measurements

Fig. 1 represents the anodic and cathodic potentiodynamic polarization of two Cu-Ni alloys in high NaCl concentration, (3.5 – 15 wt%), at room temperature. The electrochemical parameters such as corrosion potential E_{corr}, corrosion current density I_{corr}, anodic and cathodic Tafel slopes β_a and β_c respectively, and corrosion rate C.R are tabulated in Table (2, 3). It is observed that the anodic and cathodic current density curves were shifted to a higher value as the concentration of NaCl increased. This behavior could be due to the decrease in the oxide film thickness. There are two possible mechanisms describing the reduction of a film thickness of copper and its alloys in saline solutions, the dissolution precipitation mechanism and the erosion mechanism **[8].** From both mechanisms, it was concluded that a film will grow over the corroding surface if the binding force between the film and the substrates is greater than the shear force. This can be explained on the basis that the cathodic response of Cu-Ni alloy in 3.5 wt% NaCl solutions is the water reduction, which is weaker than the oxygen reduction reaction in the freely aerated solutions. The cathodic reaction consumes the electrons that are produced in the dissolution process of the anodic reaction, which is why the weaker the cathodic reaction the lower the dissolution of Cu-Ni alloys. Some in situ deep-sea environment corrosion tests showed that metal structural materials undergo serious corrosion in the deep sea environment **[1].** From Table (2, 3), it was found that, increase the concentration of NaCl leads to increase of corrosion current density and corrosion rate, accompanied with shifting the corrosion potential of the Cu-Ni alloys to more negative values. It is also indicated that the values of corrosion current density for Cu-30 Ni alloy, where higher Ni content, are less than Cu-10 Ni alloy, i.e. the I_{corr} decreased with increasing the Ni content for the two Cu-Ni alloys reaching its maximum in 15 wt% NaCl where 184.00 $\mu A/cm^2$ and 34.307 $\mu A/cm^2$ for Cu-10 Ni alloy and Cu-30 Ni alloy, respectively.

Chronoamperometric potentiostatic current-time (CT) measurements

Chronoamperometric   potentiostatic

polarization test was operated to determine the mechanism of pitting corrosion of Cu-Ni alloys in high NaCl concentration solution. Fig. (2) shows the chronoamperometric curves for two Cu-Ni alloys in high NaCl concentration measured at pitting corrosion zone (zero Volt). Investigation of Fig. (2) shows that, the current density gradually decreases with the prolongation of time which give higher stabilized passive currents at 15 wt% NaCl concentration approximately 42.156 mA/cm^2 and 14.572 mA/cm^2 for Cu-10 Ni alloy and Cu-30 Ni alloy, respectively. The chloride concentration is the most significant component in the passive current case. The immersion current density (I_{im}) and steady-state current density ($I_{s.s}$) for the two Cu-Ni alloys are given in Table (4). This information indicated that Cu-10 Ni alloy has higher passive current density than Cu-30 Ni alloy. The corrosion of Cu-Ni alloys typically starts with the removal of the passive oxide layer, followed by oxidation of the copper to different oxidation states. This process forms corroded pits, which are detected through the rapid increase of the oxidation current **[9].** It is clearly seen that the current for Cu-30Ni in high NaCl solution, Fig. (2) recorded very low values in the measurement as compared to Cu-10 Ni. This might be due to the accretion of corrosion mathematical product and/ or graduated table from seawater on the Cu-Ni control surface, which in play, partially block the surface from being attacked by the surrounding environment. Increasing the time increased the current values as a result of the aggressive ions attack present in the seawater on the flawed areas of the Cu-Ni surface leading to the occurrence of pitting corrosion. The current then decreased and stayed almost constant until the end of the experiment. The CT data thus confirmed the results obtained from the polarization measurements.

Electrochemical Impedance spectroscopy

The corrosion behaviors of two Cu-Ni alloys were investigated in high NaCl solutions by using EIS technique at room temperature. Fig. (3) shows the Nyquist and Bode plot of two Cu-Ni alloys in high NaCl (3.5 wt% - 15 wt%) concentration. The Nyquist plots show a depressed semicircle shape with their centers below the real axis. This behavior shows the frequency dispersion of the impedance data **[10].** There are several reasons for this: surface roughness, impurity, dislocation, grain boundary, etc., may cause this depressing view of Nyquist diagrams. The corroding surface of brass is expected to inhomogeneous because of its
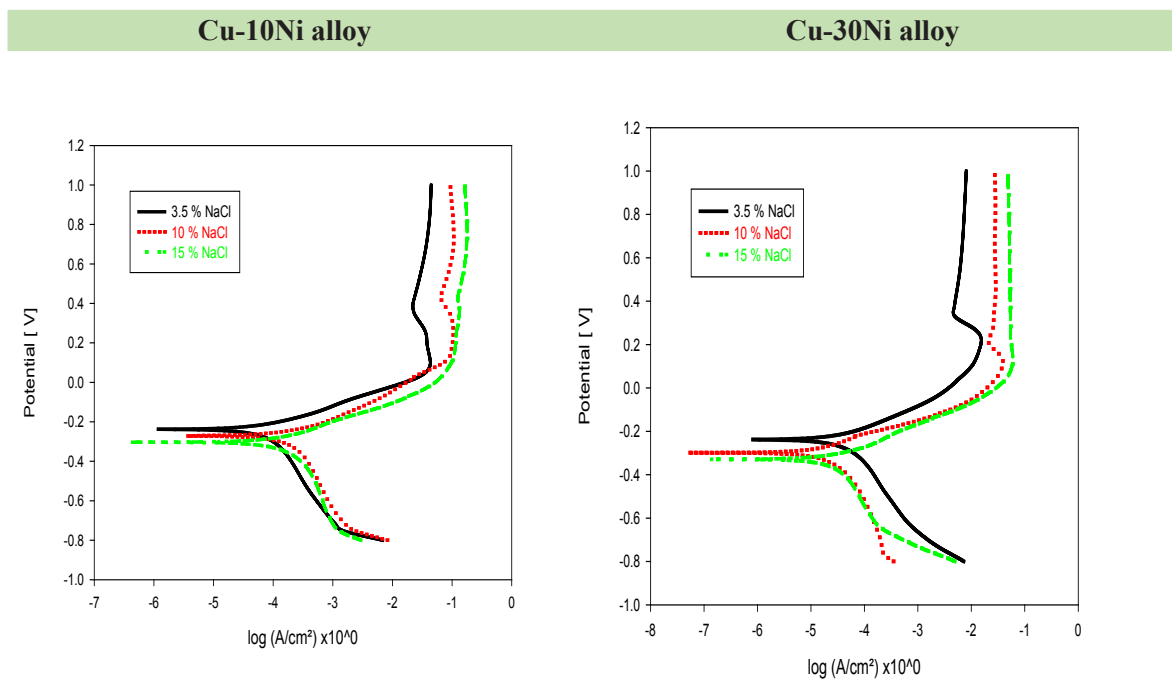
Cu-10Ni alloy	Cu-30Ni alloy

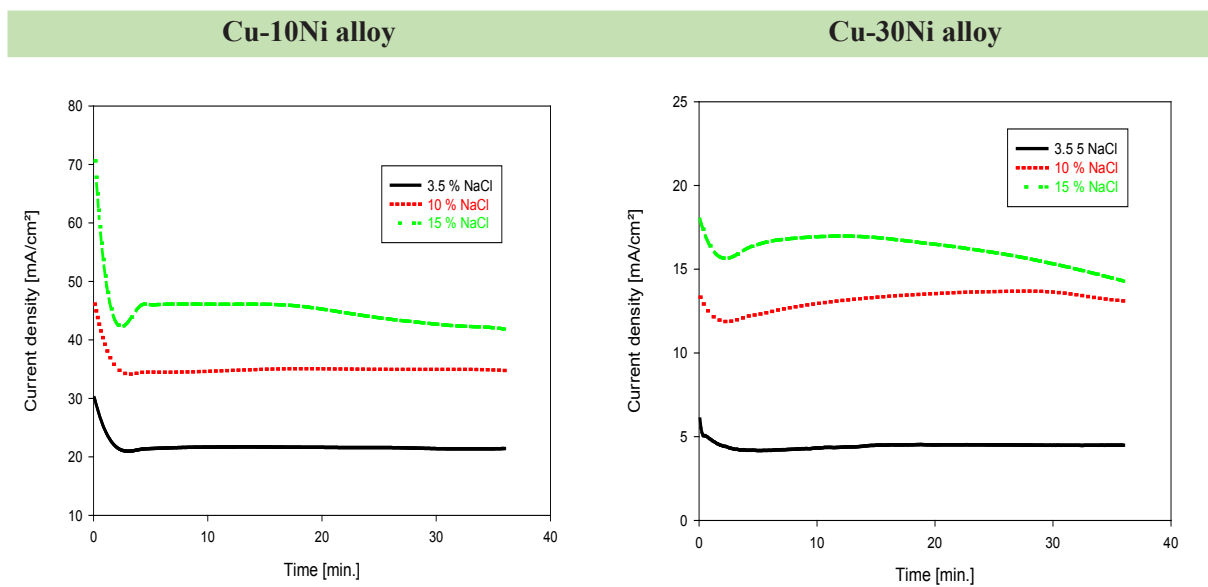**Fig. 1. Anodic and cathodic potentiodynamic polarization curve for two Cu-Ni alloys in high concentrations of NaCl, at 25 ^{0}C.**

Cu-10Ni alloy	Cu-30Ni alloy

Fig. 2. Chronoamperometric curve for two Cu-Ni alloys in high concentration of NaCl, at 25 ^{0}C.

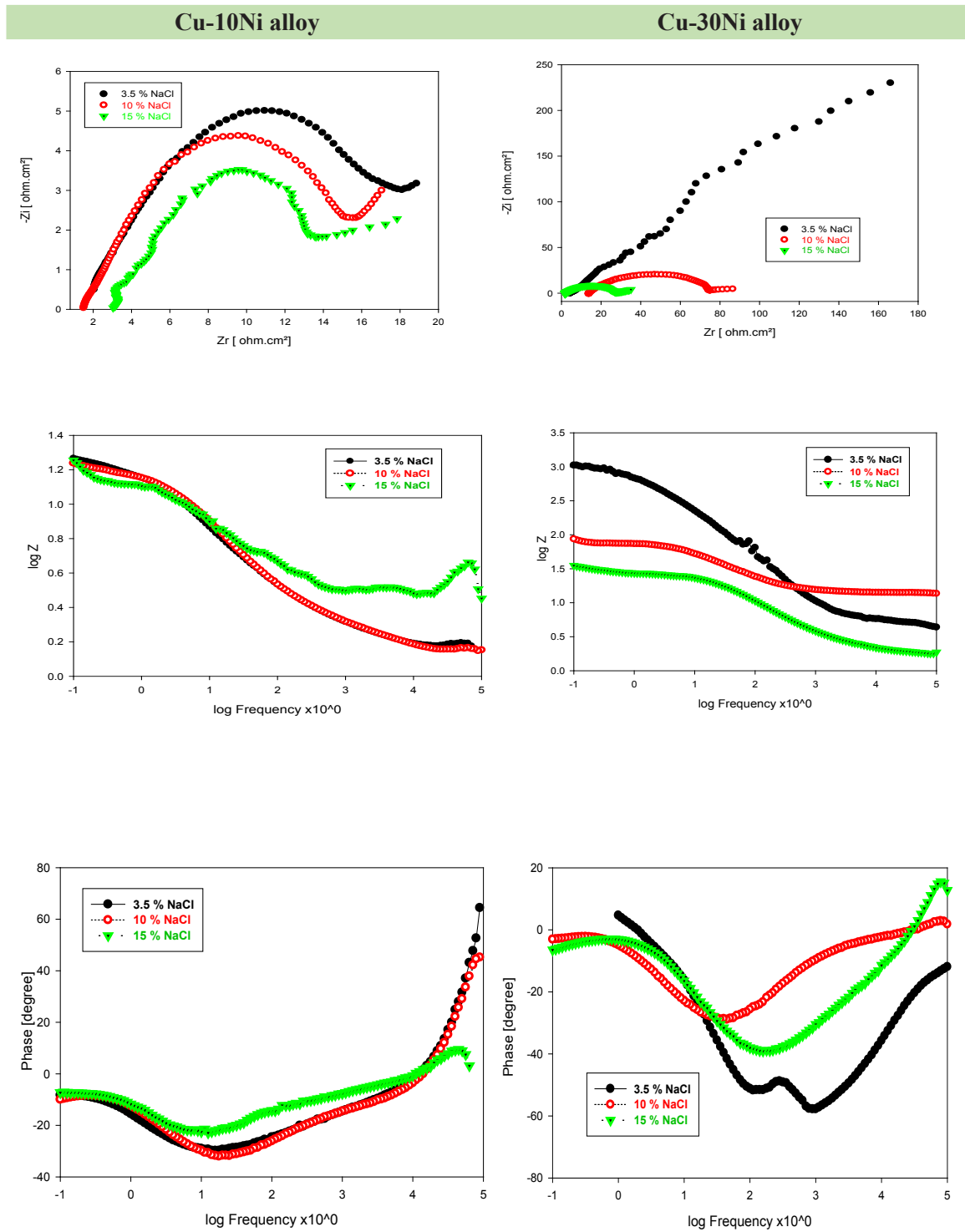**Cu-10Ni alloy**   **Cu-30Ni alloy**

Fig. 3. Nyquist and Bode plot for two Cu-Ni alloys in high concentration of NaCl, at 25 ⁰C.

roughness. Therefore, the capacitance is presented through a constant phase element (CPE) [10]. The Bode plots for the specimens after corrosion for two Cu-Ni alloys showed little difference, except for bigger |Z| values. The semicircles of the two capacitive loops were smaller. For the Bode plots in Fig. 3, the modulus (|Z|) of the impedance was also smaller. All of the results show that the compact property of corrosion products formed. For the phase angle plots, two more peaks appear indicating duplex corrosion products formation on the specimens after corrosion. The fitting results for two Cu-Ni alloys show that both of the charge transfer resistance (R_{ct}) and resistance of corrosion products under Cu-30Ni alloy were lower than that under Cu-10Ni alloy, which indicates a faster corrosion rate at high pressure in accordance with the potentiodynamic results and as anticipated from the observed morphologies of the corrosion products. The impedance parameters for the Cu-Ni alloys in high NaCl concentration such as charge transfer resistance (R_{ct}) and double-layer capacitance (C_{dl}) are given in Table (5). Inspection of these data show that the charge transfer resistance of the Cu-Ni alloys decreases while C_{dl} value increases with increasing concentration of NaCl solutions. Electrochemical theory shows that the reciprocal of the charge transfer resistance, $1/R_{ct}$, is directly proportional to the corrosion rate [11]. This means that the corrosion rate increases with increasing concentration. The corrosion rate of Cu-10 Ni alloy is higher than Cu-30 Ni alloy. The decrease in R_{ct} and increase in C_{dl} values with increase in the concentration of NaCl solution suggest an increase in the rate of corrosion of Cu-Ni alloys and support the notice mode in the potentiodynamic and chronoamperometric potentiostatic polarization studies.

Effect of temperature on Cu-Ni alloys in 3.5 wt% NaCl solution

Temperature investigations are important in corrosion studies to determine the activation energy (E_a) and calculated the dissolution process. Therefore, the corrosion rate of Cu-Ni alloys in 3.5 wt% NaCl solution was determined at different temperature for E_a calculation. The relation between corrosion rate and the temperature is given in the Arrhenius equation (1) [12]

$$C.R = A \exp^{-E_a/RT} \qquad (1)$$

where C.R is the corrosion rate of Cu-Ni alloys, A is Arrhenius constant or pre-exponential factor, R is the universal gas constant and T is absolute temperature. Linearization of equation (1) gives equation (2)

$$\ln C.R = \ln A - E_a/RT \qquad (2)$$

By using potentiodynamic polarization measurements the effect of temperature on Cu-Ni alloys in 3.5 wt% NaCl solution was studied in the temperature extent (25, 50 and 75 ^{0}C). Fig. (4) shows anodic and cathodic potentiodynamic polarization curved shape for two Cu-Ni alloys in 3.5 wt% NaCl at 25, 50 and 75 ^{0}C. The electrochemical parameters such as corrosion potential E_{corr}, corrosion current density I_{corr}, anodic and cathodic Tafel slopes β_a, and β_c respectively, and corrosion rate C.R are tabulated in Table (6, 7). It is clear from the tables that, the corrosion current density I_{corr}, for Cu-Ni alloys, increases with increasing temperature which indicates that the corrosion process is including a transport medium in the temperature range of our investigation (298 K- 348 K). Fig. (5) represents the Arrhenius plots of the ln C.R. vs. 1/T for the Cu-Ni alloys in 3.5 wt% NaCl solution. From the slopes of these plots - Ea/ R, the activation energy values were calculated and presented in Table (8). The calculated activation energy values of two Cu-Ni alloys were 4.872 and 18.512 KJ/ mol for Cu-10 Ni alloy and Cu-30 Ni alloy, respectively. The molar activation energy of an electrochemical process makes reference to the energy level that must be overcome by the electron in the exchange through the electrode/electrolyte interface. In this way, low E_a values indicate high corrosion rate values. Arrhenius indicates that the faster the dependence of the corrosion rates with the temperature the higher E_a [13, 14].

Scanning Electron Microscopy (SEM) and energy dispersive X-ray (EDX) investigations

Fig. 6 shows the SEM image and the corresponding EDX profile analysis of the surface of two Cu-Ni alloys after 72 h submerging in 3.5 wt% NaCl solution. These figures clearly display that the surface is severely corroded and there is a formation of different forms of corrosion products on the alloy surface. For the two Cu-Ni alloys in 3.5 wt% NaCl that the surface appearance flat surface area covered with some corrosion product in plus to a wide pit, which is also covered with corrosion products. This proves that surface pitting corrosion when exposed to 3.5 wt% NaCl. The atomic percentages of the

TABLE 1. Chemical composition (wt. %) of two Cu-Ni alloys

Alloy	Alloying elements						
	Cu	Ni	Fe	Mn	Sn	Ca	Si
Cu-10 Ni	88.24	9.27	1.67	0.768	--	--	--
Cu-30 Ni	69.53	29.16	0.023	--	0.139	0.508	0.442

TABLE 2. Corrosion parameters for Cu-10Ni alloy in high concentration of NaCl, at 25 ⁰C.

Cu-10Ni alloy	E_{corr} mV	I_{corr}	βa	βc	C.R. μm/y
		μA/cm²	mV	mV	
3.5 %	-242.9	45.91	80.7	-186.2	531.7
10 %	-276.2	119.94	115.2	-248.2	1389
15 %	-308.2	184.00	118.0	-400.2	2131

TABLE 3. Corrosion parameters for Cu-30Ni alloy in high concentration of NaCl, at 25 ⁰C.

Cu-30Ni alloy	E_{corr} mV	I_{corr}	βa	βc	C.R. μm/y
		μA/cm²	mV	mV	
3.5 %	-241.1	10.028	87.3	-128.9	116.0
10 %	-303.6	29.209	97.7	-185.3	338.3
15 %	-334.1	34.307	114.0	-416.6	397.4

TABLE 4. Values of I_{im} and $I_{s.s}$ for Cu-Ni alloys in high concentration NaCl solution, at 25 ⁰C.

Conc. of NaCl	Cu-10Ni alloy		Cu-30Ni alloy	
	I_{im}	$I_{s.s}$ mA/cm²	I_{im} mA/cm²	$I_{s.s}$
	mA/cm²			mA/cm²
3.5 %	30.100	21.225	6.051	4.369
10 %	46.138	35.111	13.337	13.252
15 %	72.306	42.156	17.986	14.572

TABLE 5. Impedance parameters for Cu-Ni alloys in high concentration of NaCl, at 25 ⁰C.

Conc. of NaCl	Cu-10Ni alloy			Cu-30Ni alloy		
	R_{ct}	C_{dl}	Phase angle	R_{ct}	C_{dl}	Phase angle
	ohm.cm²	mF/cm²		ohm.cm²	mF/cm²	
3.5 %	54.99	2.893	-20.4	110.7	1.437	-12.2
10 %	16.52	3.029	-16.7	64.79	2.200	-12.4
15 %	11.76	3.469	-10.6	28.59	2.226	-13.8

TABLE 6. Corrosion parameters for Cu-10Ni alloy in 3.5 % NaCl solution, at 25, 50 and 75 ⁰C.

Cu-10Ni alloy	E_{corr} mV	I_{corr}	βa	βc	C.R. μm/y
		μA/cm²	mV	mV	
25 ⁰C	-242.9	45.91	80.7	-186.2	531.7
50 ⁰C	-278.8	59.33	57.4	-57.9	687.3
75 ⁰C	-307.1	60.55	231.6	-175.1	701.4

TABLE 7. Corrosion parameters for Cu-30Ni alloy in 3.5 % NaCl solution, at 25, 50 and 75 ^{0}C.

Cu-30Ni alloy	E_{corr} mV	I_{corr}	βa	βc	C.R. µm/y
		µA/cm²	mV	mV	
25 ^{0}C	-241.1	10.028	87.3	-128.9	116.0
50 ^{0}C	-263.9	27.059	81.6	-137.1	313.4
75 ^{0}C	-292.4	28.663	80.1	-119.6	332.0

TABLE 8. Activation Energy E_a for Cu-Ni alloys in 3.5% NaCl solution.

Alloy	Slop	Pre-exponential factor (A)	Linear regression coefficient (r^2)	E_a (kJ/mole)
Cu-10Ni alloy	-586.019	2.113	0.838817	4.872
Cu-30Ni alloy	-2226.65	2.514	0.826101	18.512

TABLE 9. The atomic percentage of elements presents on the Cu-Ni alloys in 3.5 % NaCl solution.

Elements %	Cu-10Ni alloy	Cu-30Ni alloy
	Blank	Blank
Cl	0.55	0.74
O	3.61	4.48
Fe	1.81	--
Ni	8.69	32.23
Cu	85.35	62.54

elements found in the selected area of SEM image by the EDX profile appearance in Table (9).The low contents of O and Cl⁻ suggest that the alloy surface is covered with corrosion products that have different chemical compound, complexes, and oxides. The comportment of chloride and iron also suggest that the surface is having scales deposited from the seawater. It is worthy to mention also that the elements found interior the pit was very high copper content and very low Ni content, which confirms the selective dissolution of Ni with copper enrichment. It was also found that the presence of oxygen inside the pit was poor compared to its percentages on the surface and around the pit. This specifies that aggressive ions such as Cl⁻ displace the oxygen at its weakest bond with metal on the alloy surface and initiate pitting corrosion. The presence of Cl⁻ at such content raises the potential difference across the passive film, thereby enhancing the rate of nickel ions diffusion from the nickel-film interface to the film-solution interface, forming cation vacancies at the Cu-Ni film interface [15]. Some authors have reported that as long as the Ni content in the copper-nickel alloy does not exceed 40 wt%, the Ni compounds would hardly appear in the corrosion product formed in Cl⁻ containing solutions [1]. Also it has been suggested that nickel ions can be incorporated in the Cu oxides as dopants, hence, nickel compounds can hardly be identified through this method. Copper peaks in the pattern indicate that pure copper existed in the corrosion products, which has also been reported by some other studies on the corrosion behavior of Cu and its alloys [16]. On the other hand and in order to see the surface morphology and to identify the composition of the species formed on the Cu-30 Ni surface after its immersion in 3.5 wt% NaCl for 72 h, it is clearly seen from the SEM image there are black and white areas with no pits observed on the Cu-Ni surface. This may indicate also that the white color presented on the surface is probably for NaCl salt, while the black areas contain the main component of the alloy. SEM/EDX investigations thus confirm that Cu-10 Ni is more corrosive towards Cu-30 Ni compared to 3.5 wt% NaCl, which also confirm the data obtained by polarization, chronoamperometry, and EIS.

Mechanism of corrosion

The corrosion behavior of Cu-Ni alloys in a neutral chloride solution is mainly redox [2]; in the chloride solution, Cl⁻ can more easily react with Cu⁺ than OH⁻ at the same concentration [17].

Therefore, Cl⁻ is the main factor responsible for corrosion of Cu or Cu alloys in sea water. The dissolution process of the copper-nickel alloy can be interpreted as follows:

The cathodic reaction occurs with the reduction of oxygen, and the anode reaction is the dissolution of copper [2].
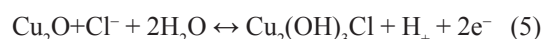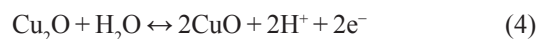
The cathodic reaction process is:

$$O_2 + 2H_2O + 4e^- \leftrightarrow 4OH^- \qquad (1)$$

The anodic reaction is the dissolution of copper form to cuprous dichloride anion ($CuCl_2^-$) which is thought to be the main dissolution process in seawater or NaCl solution [18, 19]:

$$Cu + 2Cl^- \leftrightarrow CuCl_2^- + e^- \qquad (2)$$
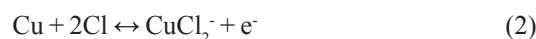
The local concentration of $CuCl_2^-$ increases at the surface leading to a hydrolysis reaction and the formation of Cu_2O according to [20, 21]:

$$2CuCl_2^- + 2H_2O \leftrightarrow Cu_2O + 4Cl^- + 2H^+ \qquad (3)$$
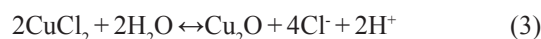
According to the Pourbaix diagram of Cu [22], in sea water at the temperature of 25 °C, under the experimental conditions, the Cu_2O still has a potential to be oxidized to CuO or $Cu_2(OH)_3Cl$ at the surface of the corrosion products through the Eqs. (4) and (5):

$$Cu_2O + H_2O \leftrightarrow 2CuO + 2H^+ + 2e^- \qquad (4)$$

$$Cu_2O + Cl^- + 2H_2O \leftrightarrow Cu_2(OH)_3Cl + H_+ + 2e^- \qquad (5)$$

As reported [23], in a highly concentrated chloride solution, local acidification within pores of the corrosion products can easily happen, which means that Eq. (5) is dominant during the re-oxidation process of Cu_2O. The Cu_2O has p-type semiconductor defects. The Cu_2O content on the surface of the sample decreases, and the content of CuO and $Cu(OH)_2$ increases, which reduces electron conductivity and improves corrosion resistance.

The further oxidation of Cu can be written as:

$$Cu_2O + O_2 + H_2O \leftrightarrow 2CuO + H_2O_2 \qquad (6)$$

$$Cu_2O + 3H_2O \leftrightarrow 2Cu(OH)_2 + 2H^+ + 2e \qquad (7)$$

Nickel is oxidized to form a dense oxide film,

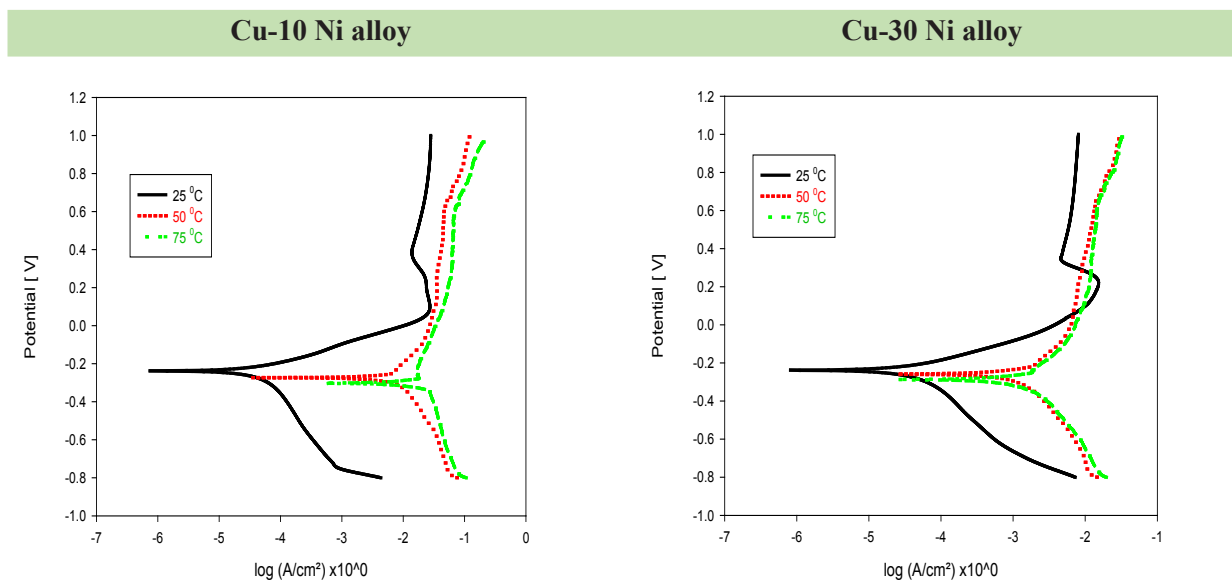| Cu-10 Ni alloy	Cu-30 Ni alloy

Fig. 4. Anodic and cathodic Potentiodynamic polarization curve for two Cu-Ni alloys in 3.5 wt% NaCl solution, at 25, 50 and 75 ^{0}C.
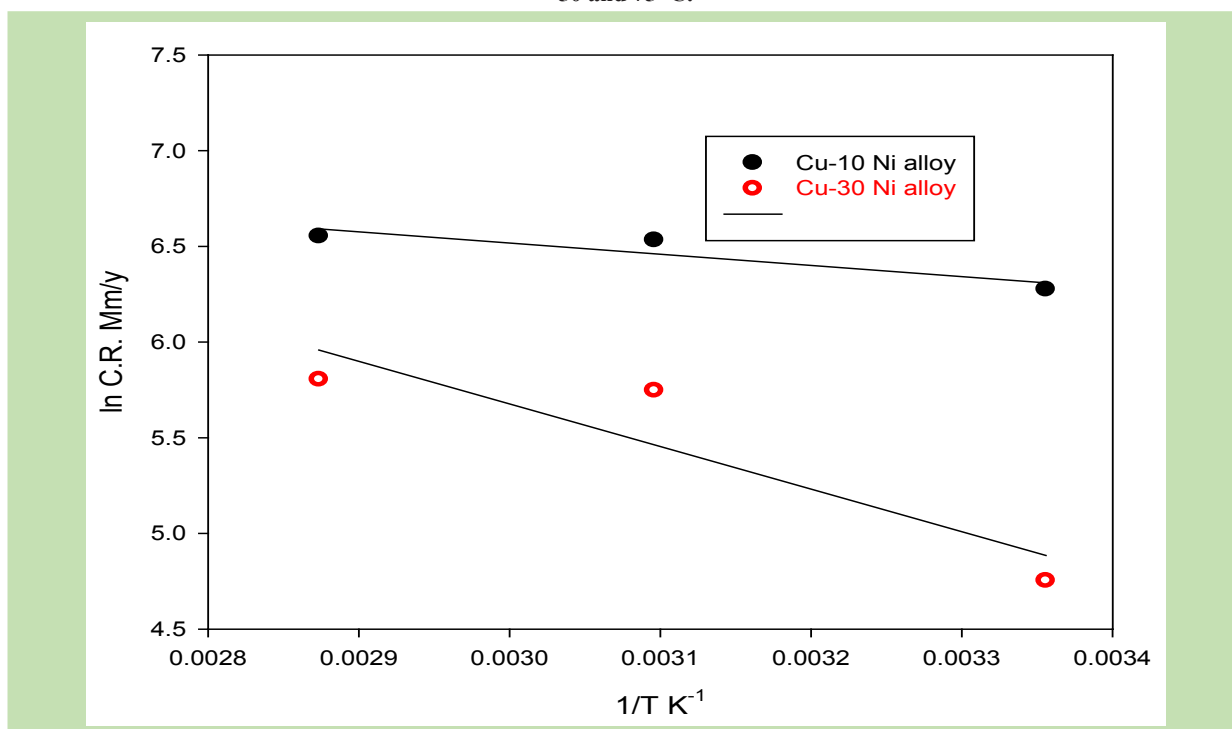

Fig. 5. Arrhenius plots of ln C.R vs. (1/T) for two Cu-Ni alloys in 3.5 wt% NaCl solution.
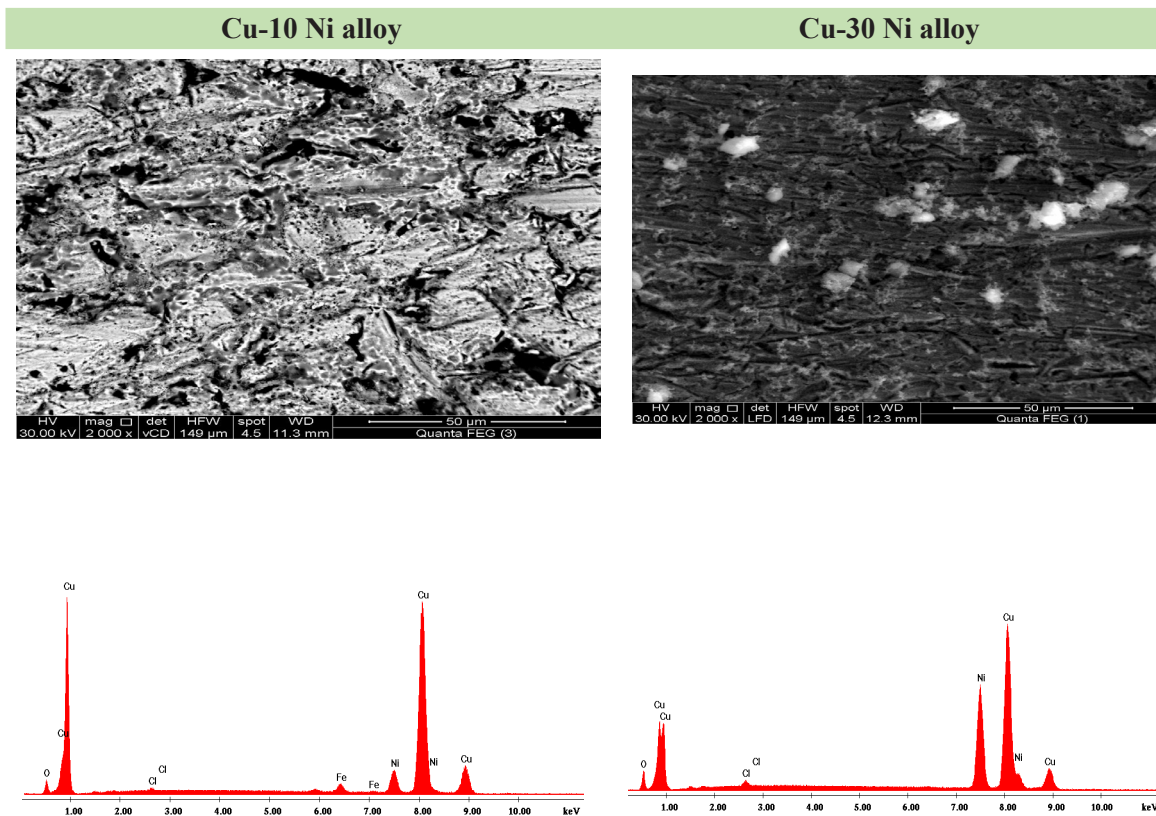
Fig. 6. SEM picture and the corresponding EDX spectra for two Cu-Ni alloys after 72 h immersion in 3.5 wt% NaCl solution.
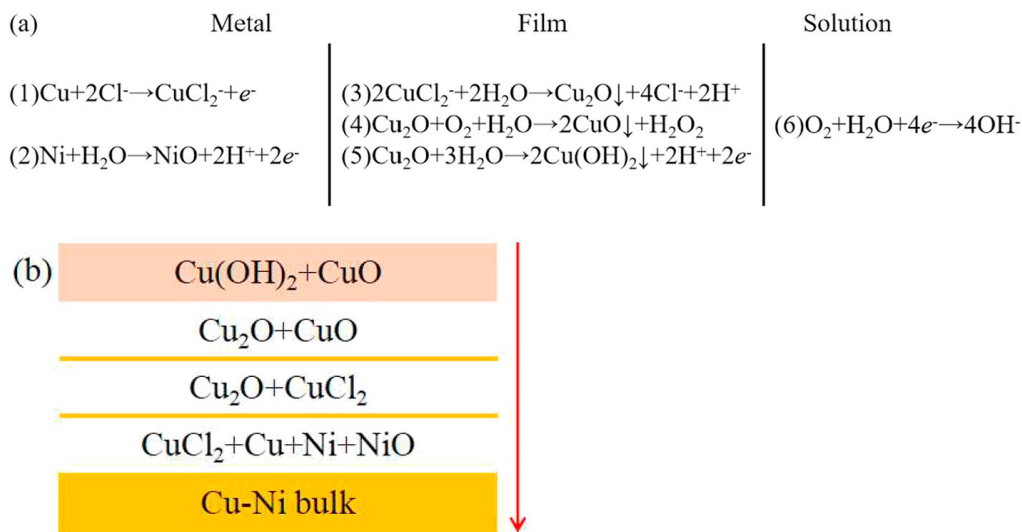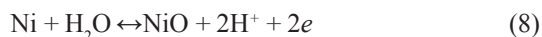

Fig. 7. (a) Schematic representation of the corrosion reaction processes that occur within a Cu-Ni alloy and (b) the chemical composition of the surface layers.

which prevents the corrosion of the alloy to some extent, and can be written as **[2]:**

$$Ni + H_2O \leftrightarrow NiO + 2H^+ + 2e \qquad (8)$$

The six basic reactions are shown in Fig. 7 (a). All of these results lead to a schematic representation of the chemical composition of the surface layers at different depths in the Cu - Ni alloy, as shown in Fig. 7 (b). The oxygen ions immediately react with the metal to form oxides to produce chemically active oxygen to further accelerate the chemical reaction between the ions of metal and oxygen at the oxide-metal interface. With the increase in treatment time the oxide film grows outwardly producing a thick layer on the alloy surface **[24, 25].** Therefore, enhancing corrosion resistance of Cu-Ni alloy in a 3.5 wt% NaCl solution can be the rate of nickel ions diffusion from the nickel-film interface to the film-solution interface, forming cation vacancies at the Cu-Ni film interface.

Conclusions

The corrosion behavior of Cu-Ni alloys in brine solutions has been studied at room temperature by using different electrochemical and spectroscopic test methods. The outcome results can be summarized as follows:

1. Polarization measurements indicated that corrosion occurred on Cu-Ni alloys in high NaCl solutions due to the attack of corrosive species such as Cl⁻ and that a selective dissolution of Ni leads to the diffusion of the formed pits.

2. Polarization tests also stated that Cu-10 Ni alloy is more corrosive than Cu-30 Ni alloy.

3. Current-time curves recorded for the Cu-Ni alloys revealed that decreases both pitting and general corrosion.

4. Electrochemical impedance spectroscopy confirmed the polarization and current-time, where the surface and polarization resistances recorded higher values in NaCl, which indicates that Cu-10 Ni alloy, is more corrosive than Cu-30 Ni alloy.

5. SEM images and EDX profiles indicated that pitting corrosion occurs faster for Cu-10 Ni alloy in 3.5 % NaCl solution and the surface develops a mixture of oxides, chlorides, and/or oxy-chloride complexes with a selective dissolution of Ni.

References

1. Hu S., Liu L., Cui Y., Li Y., and Wang F., Influence of hydrostatic pressure on the corrosion behavior of 90/10 coppernickel alloy tube under alternating dry and wet condition Corrosion Science, 146, 202–212, (2019).

2. Xia T., Zeng L., Zhang X., Liu J., Zhang W., Liang T., and Yang B., Enhanced corrosion resistance of a Cue10Ni alloy in a 3.5 wt% NaCl solution by means of ultrasonic surface rolling treatment Surface & Coatings Technology, 363, 390–399, (2019).

3. Abu-Eid Z.M., and Fakhoury A.G., Some special design features of Kuwait MSF plants, Desalination, 23, 263-284, (1974).

4. Ghayad I. M., Abdel Hamid Z., and Gomaa N., A Case Study: Corrosion Failure of Tube Heat Exchanger, Journal of Metallurgical Engineering (ME), 4, 57-61, (2015).

5. Fouda A. S., Elewady G. Y., and Salama M. G., Enaminonitrile derivatives as corrosion inhibitors for Cu10Ni alloy in 0.5 M HCl solutions, Der Pharma Chemica, 5 (4), 20-30, (2013).

6. Hurtado M. R. F., Sumodo P.T. A. and Benedtti A. V., Electrochemical studies with a Cu-5wt.%Ni alloy in 0.5 M H_2SO_4, Electrochimica Acta, 48, 2791-2798, (2003).

7. Gonçalves R. S., Azambuja D. S., Serpa Lucho A. M., Reche M. P. and Schmidt A. M., Electrochemical Studies of Copper, Nickel and a Cu55/Ni45 Alloy in Aqueous Sodium Acetate, Materials Research, 4 (2), 97-101, (2001).

8. Nagiub A.M., Evaluation of corrosion behavior of copper in chloride media using electrochemical impedance spectroscopy (EIS), Portug. Electrochimica Acta, 22, 301-314, (2005).

9. Arjmand F. and Adriaens A., Influence of pH and Chloride Concentration on the Corrosion Behavior of Unalloyed Copper in NaCl Solution: A Comparative Study Between the Micro and Macro Scales, Materials, 5, 2439-2464, (2012).

10. Almzarzie Kh., Falah A., Massri A. and Kellawi H., Electrochemical Impedance Spectroscopy (EIS) and Study of Iron Corrosion Inhibition by Turmeric Roots Extract (TRE) in Hydrochloric Acid Solution, Egypt. J. Chem. 62 (3), 501 – 512,

(2019).

11. Ghanem W. A., Ahmed A. S. I., Hussein W. A., and Gaber Gh. A., Electrochemical Behavior and Effect of Temperature on Dezincification of Cu-Zn Alloys in Brine Solutions, International Journal of Metallurgical & Materials Science and Engineering (IJMMSE), 6 (4), 1-16, (2016).

12. Khadom A.A., Effect of temperature on corrosion inhibition of copper-nickel alloy by tetra ethylenepentaamine under flow conditions, J. Chil. Chem. Soc., 59 (3), 2545-2549, (2014).

13. Gaber Gh. A., Maamoun M. A., and Ghanem W. A., Evaluation of the Inhibition Efficiency of a Green Inhibitor on Corrosion of Cu-Ni Alloys in the Marine Application, Key Engineering Materials, 786, 174-194, (2018).

14. El-Sherif R.M., Ismail K.M. and Badawy W.A., Effect of Zn and Pb as alloying elements on the electrochemical behavior of brass in NaCl solutions, Electrochemica Acta , 49, 5139-5150, (2004).

15. Sherif E. M., Almajid A. A., Bairamov A. K., and Al-Zahrani E., A comparative Study on the Corrosion of Monel-400 in Aerated and Deaerated Arabian Gulf Water and 3.5% Sodium Chloride Solutions, Int. J. Electrochem. Sci., 7, 2796 – 2810, (2012).

16. Ma A., Jiang S., Zheng Y., and Ke W., Corrosion product film formed on the 90/10 copper–nickel tube in natural seawater: Composition/structure and formation mechanism, Corrosion Science, 91, 245–261, (2015).

17. Sun B., Ye T., Feng Q., Yao J., and Wei M., Accelerated Degradation Test and Predictive Failure Analysis of B10 Copper-Nickel Alloy under Marine Environmental ConditionsMaterials, 8, 6029–6042, (2015).

18. Neodo S., Carugo D., Wharton J.A., and Stokes K.R., Electrochemical behavior of nickel–aluminium bronze in chloride media: Influence of pH and benzotriazole, Journal of Electroanalytical Chemistry , 695, 38–46, (2013).

19. Krogstad H.N., and Johnsen R., Corrosion properties of nickel-aluminium bronze in natural seawater—Effect of galvanic coupling to UNS S31603, Corrosion Science, 121, 43–56, (2017).

20. Badawy W.A., El-Rabiee M., Helal N.H. and Nady H., The role of Ni in the surface stability of Cu–Al–Ni ternary alloys in sulfate–chloride solutions, Electrochimica Acta, 71, 50–57, (2012).

21. El Warraky A.A., El Meleigy A. E. and Abd El Hamid Sh. E., The Electrochemical Behavior of 70-30 Cu-Ni Alloy in LiBr Solutions, Egypt. J. Chem. 59 (5), 833- 850, (2016).

22. Bianchi G., and Longhi P., Copper in sea-water, potential-pH diagrams, Corrosion Science, 13, 853–864, (1973).

23. Campbell S.A., Radford G.J.W., Tuck C.D.S., and Barker B.D., Corrosion and Galvanic Compatibility Studies of a High-Strength Copper-Nickel Alloy, Corrosion, 58, 57–71, (2002).

24. Chenakin S.P., Mordyuk B.N., and Khripta N.I., Surface characterization of a ZrTiNb alloy: Effect of ultrasonic impact treatment, Applied Surface Science, 470, 44–55, (2019).

25. Vasylyev M.A., Chenakin S.P., and Yatsenko L.F., Ultrasonic impact treatment induced oxidation of Ti6Al4V alloy, Acta Materialia, 103, 761–774, (2016).

دراسة مقارنة للتآكل الكهروكيميائي للتصميمات الجديدة لـ 90/10 و 70/30 من سبائك النحاس - **نيكل**
في المحاليل الملحية

غالية أسعد جابر ، ولاء أحمد حسين ، أمال صلاح ابراهيم أحمد

قسم الكيمياء ، كلية العلوم (بنات) ، جامعة الأزهر ، مدينة نصر ، القاهرة ، مصر.

تعد سبائك النحاس - نيكل هي المادة المفضلة فى العمليات الصناعية وخاصة المكثفات والمبادلات الحرارية ، حيث يتم استخدام مياه البحر كمبرد في محطات تحلية المياه وتعمل سبائك النحاس أيضا فى أوساط المياه المالحه ومياه النيل التى تحتوى على الكلوريدات التى تسبب التآكل . في هذا البحث ، قمنا بمقارنة سلوك التآكل للتصميمات الجديدة لسبائك النحاس - نيكل بنسبة 90/10 و 70/30 تحت درجة ملوحة عالية (3.5٪ بالوزن ، 10٪ بالوزن و 15٪ بالوزن من كلوريد الصوديوم). تمت دراسة التآكل الكهروكيميائي لسبائك Cu-Ni في المحاليل الملحية باستخدام الجهد الديناميكى الحركى ، Chronoamperometric وطريقة المعاوقة الكهروكيميائيه بالإضافة إلى الميكروسكوب الالكترونى الماسح (SEM) والتحليل المشتت بالأشعة السينية (EDX). أظهرت نتائج الاستقطاب أن سبيكة Cu-10 Ni أكثر تآكلًا من سبيكة Cu-30 Ni في محلول كلوريد الصوديوم بنسبة 3.5٪ بالوزن. وأكدت منحنيات ال Chronoamperometric النتائج التي تم الحصول عليها عن طريق قياسات الجهد الديناميكى الحركى بأن التآكل لسبائك Cu-Ni قد انخفض في سبيكة Cu-30 Ni في محلول كلوريد الصوديوم بنسبة 3.5٪ بالوزن. كشفت نتائج المعاوقة الكهروكيميائيه أن مقاومة السطح والاستقطاب سجلت قيمًا أعلى في سبيكة Cu-30Ni. أشارت الفحوصات التي أجريت بواسطة EDX / SEM إلى أن تآكل سبائك النحاس - نيكل استمر في الذوبان الكهربائي ، مما يسمح بترسيب النحاس على سطح السبائك. ويدل هذا إلى قابلية حدوث تأكل التنقر.